Elementary Supplementary Document

Bifunctional Sr(II)-Based Coordination Polymer for Sensing of Ba(II)/Nitro-aromatic Compounds and Supercapacitor Applications

Shama Firdaus[a], Waris[b], Mohd Tameem[a], Arif Ali[c], Sumra Dilshad[a], Musheer Ahmad[a], Mohammad Zain Khan[b], Farman Ali[a] and Aiman Ahmad[a]*

[a]Department of Applied Chemistry, ZHCET, Faculty of Engineering and Technology, Aligarh Muslim University, Aligarh, UP–202002, India

[b]Electrochemical Research Laboratory, Department of Industrial Chemistry, Faculty of Science, Aligarh Muslim University, Aligarh, UP–202002, India

[c]Department of Chemistry & Chemical Biology, Indian Institute of Technology (ISM), Dhanbad, Jharkhand- 826004, India

*Corresponding author:

E–mail address: aiman.ahmad1@gmail.com (Aiman Ahmad) Tel.: +91-9456466879

Contents

1. Experimental Section

1.1. Materials and Reagents

1.1.1. For SA2 CP: 3,5-pyridine dicarboxylic acid [$C_7H_5NO_4$] (3,5-PDC) and strontium nitrate [$Sr(NO_3)_2$] were purchased from Sigma Aldrich and used as received. The solvents DMF, Ethanol and acetic acid were obtained from Thermo Fisher scientific, India and used without any further purification.

1.1.2. For rGO: the base chemical of analytical grade pure graphite powder was purchased from Sigma Aldrich. Sulfuric acid (H_2SO_4), sodium nitrate ($NaNO_3$), potassium permanganate ($KMnO_4$), sodium borohydride ($NaBH_4$), acetone and hydrogen peroxide (H_2O_2) were acquired from Thermo Fisher scientific, India.

Nitroaromatic compounds and nitrate salts of metal were procured from Sigma Aldrich and used as received and double distilled water was used throughout the work.

1.2. Physical Measurements: SA2 elemental analysis was obtained from a CE-440 elemental analyzer (Exeter Analytical Inc.). SA2, rGO, and rGO@SA2 infrared spectra were recorded using the Thermo Scientific iS50 FTIR in the range of 4000–400 cm^{-1} using KBr disc, and powder X-ray diffraction (PXRD) were recorded using a Miniflexll X-ray diffractometer with Cu Kα radiation at a scan rate of $5^o min^{-1}$ at 298 K in the range of 5º-50º at 40 kV and 30 mA. From an open capillary procedure, their melting point was determined. Solid-state ^{13}C NMR was obtained from a JEOL JNM-ECX Series 400 MHz NMR spectrometer that was mounted with a solid-state multinuclear MAS probe. Using Cross Polarization Magic Angle Spinning (CP/MAS) SA2 was spun at a Magic Angle Spinning (MAS) speed of 10 kHz. Chemical shifts were measured in parts per million (ppm). Thermal study (thermalgravimetric analysis) of SA2, rGO and rGO@SA2 were performed on a TGA-50H instrument. The morphologies of the synthesized materials were studied using SEM with a JSM-6510 (0.5-1 kV) model instrument and TEM with a TECHNAI 200 kV (Fei, Electron Optics) instrument coupled with a 35 mm photography system and digital imaging equipment. Perkin Elmer λ-45 UV visible spectrophotometers with a 1 cm path length were used to determine the electronic spectrum of compounds in water 10^{-3} M solutions. Emission spectra were recorded using the Hitachi F-2700 spectrophotometer. SA2 and rGO@SA2 electrochemical charge-discharge capacity were measured at room temperature using a potentiostat (PGSTAT204 N, Metrohm Autolab, Netherlands) fitted with a set of three electrode system.

1.3. Single Crystal X-ray Data and Topological Analysis: A Bruker SMART APEX CCD diffractometer at 100 K was used to collect single-crystal X-ray data of SA2 CP with graphite monochromatic and Mo-Kα radiation (λ = 0.71073 Å). The data reduction and integration were performed using SAINT software, empirical absorption correction was performed using SADABS software, and the space group analysis was conducted using XPREP software. Determination and the refinement of the crystal structure was done by Olex2 software [1] and olex2.refine refinement package [2], respectively. In the structure, hydrogen atoms were refined isotropically and located in distinct Fourier maps, whereas all non-hydrogen atoms were refined with anisotropic displacement parameters. The ToposPro software suite and the TTD collection of periodic networks provided the topology data for the construction.[3] The nets were identified using Topos NDn nomenclature [4], and the order of the atoms in the structures was ascertained using the AutoCN program's "Domains" technique.[5] 2244068 is the CCDC reference number for SA2.

2. Photoluminescence Performance Analysis

Using fluorescence-quenching titration, the potential application of SA2 for the detection of small amounts of aromatic compounds particularly those containing carboxylic acid functional groups or nitro groups and certain metal ions was investigated. The following equation was used to determine the luminescence quenching efficiency (Q):[6]

$$Q(\%) = \{\frac{I_o - I}{I_o}\} \times 100$$

where, the luminescence emission intensity before the addition of solvents or metal ions is denoted by I_o, while after the addition is denoted by I.

Further, to measure the strength of the complex formed between a fluorophore and analytes, the formation constant (Ksv) was determined using the equation:[6]

$$\frac{F_o}{F} = 1 + K_{sv}[Q]$$

Where F and F_o are the fluorescence intensity with and without quencher, respectively, K_{sv} is the complex formation constant (litre/mole) for quenching, and [Q] is the quencher concentration (mole/litre). The above equation is similar to the Stern-Volmer equation except that it gives formation constant rather than Stern-Volmer constant, which is related to dynamic quenching as well as static quenching. The fluorescence intensities were measured at the peak emission wavelengths. The K_{sv} is calculated from the slope of the linear fit between the quenching and quencher concentration. A higher K_{sv} value indicates stronger interaction and increased complex stability. The minimum detection limit was also calculated using the formula **Limit of detection (LOD) = 3s/m** [7], where s is the standard error and m is the slope showing the sensitivity of the photoluminescence experiment. A lower LOD indicates higher sensitivity, or the capacity of the method to detect lower quantities of analytes.[8]

3. Electrochemical Performance Analysis

Using cyclic voltammetry (CV) at scan rates between 10-500 mVs^{-1}, with a potential window of +0.15 to +1.0 V (vs. Ag/AgCl), measuring galvanic charge-discharge (GCD) at current densities between 1.0 Ag^{-1} and 6.0 Ag^{-1} within the same potential window, and electrochemical impedance spectroscopy (EIS) over a frequency range of 0.1 Hz to 100 kHz, with a 10 mV amplitude, the electrochemical properties of the fabricated electrodes were analysed in 1.0 M H_2SO_4 aqueous electrolyte solution.

To determine the specific capacitance of SA2 and rGO@SA2 equation (1) is used, as shown below:[9]

$$C_p = \frac{(I \times \Delta t)}{m \times \Delta V} \quad \dots (1)$$

where C_p is the specific capacitance in Fg^{-1}, I is the constant discharge current, Δt is the discharge duration, m is the mass of the electroactive material and ΔV is the potential window.

4. Table ES1: Crystal data and structure refinement for SA2.

Identification code	2244068
Empirical formula	$C_7H_7NO_6Sr$
Formula weight	288.75
Temperature/K	293(2)
Crystal system	triclinic
Space group	P-1
a/Å	7.91410(10)
b/Å	8.00640(10)
c/Å	8.08520(10)

α/°	88.6280(10)
β/°	71.2940(10)
γ/°	72.0430(10)
Volume/Å^3	460.008(11)
Z	2
ρ_{calc} g/cm^3	2.0845
μ/mm^{-1}	5.869
F(000)	281.0
Crystal size/mm^3	0.37 × 0.21 × 0.14
Radiation	Mo Kα (λ = 0.71073)
2Θ range for data collection/°	5.34 to 54.76
Index ranges	$-10 \leq h \leq 10$, $-10 \leq k \leq 10$, $-10 \leq l \leq 10$
Reflections collected	26681
Independent reflections	2007 [R_{int} = 0.0492, R_{sigma} = 0.0239]
Data/restraints/parameters	2007/0/146
Goodness-of-fit on F^2	1.051
Final R indexes [I>=2σ (I)]	R_1 = 0.0188, wR_2 = 0.0425
Final R indexes [all data]	R_1 = 0.0210, wR_2 = 0.0430
Largest diff. peak/hole / e Å^{-3}	0.37/-0.33

5. Powder X-Ray Diffraction (PXRD)

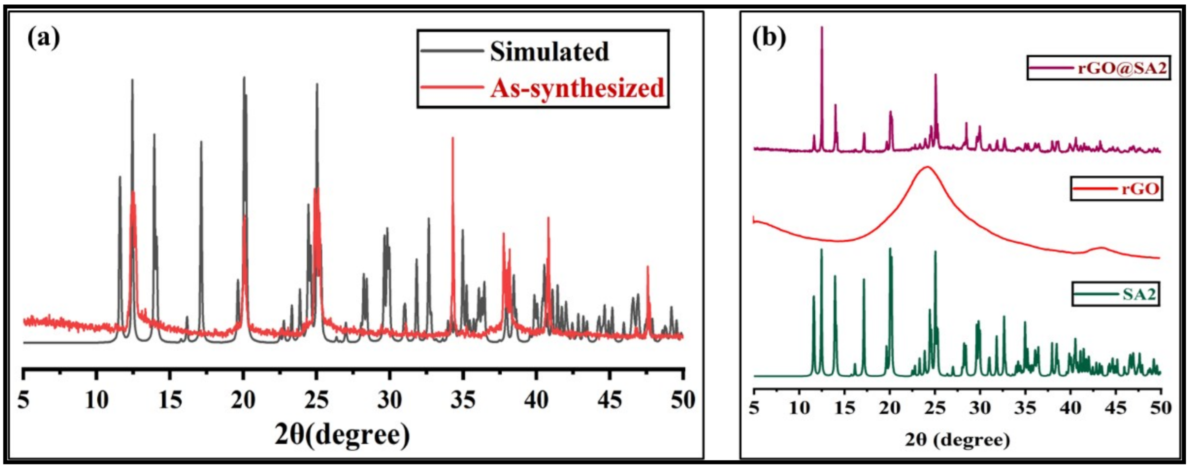

Figure ES1. (a) SA2 simulated and as-synthesized PXRD patterns of SA2 and **(b)** PXRD pattern of SA2, rGO and rGO@SA2

6. Fourier Transform Infra-Red Spectra (FT-IR)

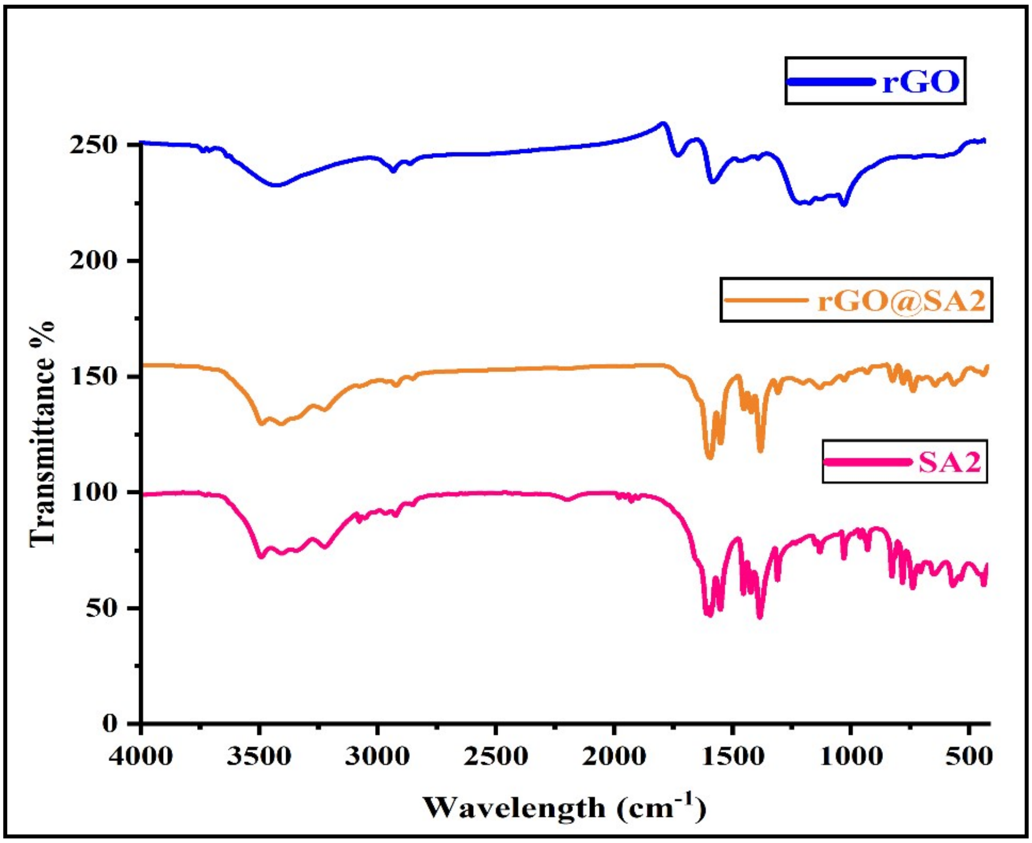

Figure ES2. FT-IR spectrum of SA2, rGO and rGO@SA2

7. Thermogravimetric Analysis (TGA)

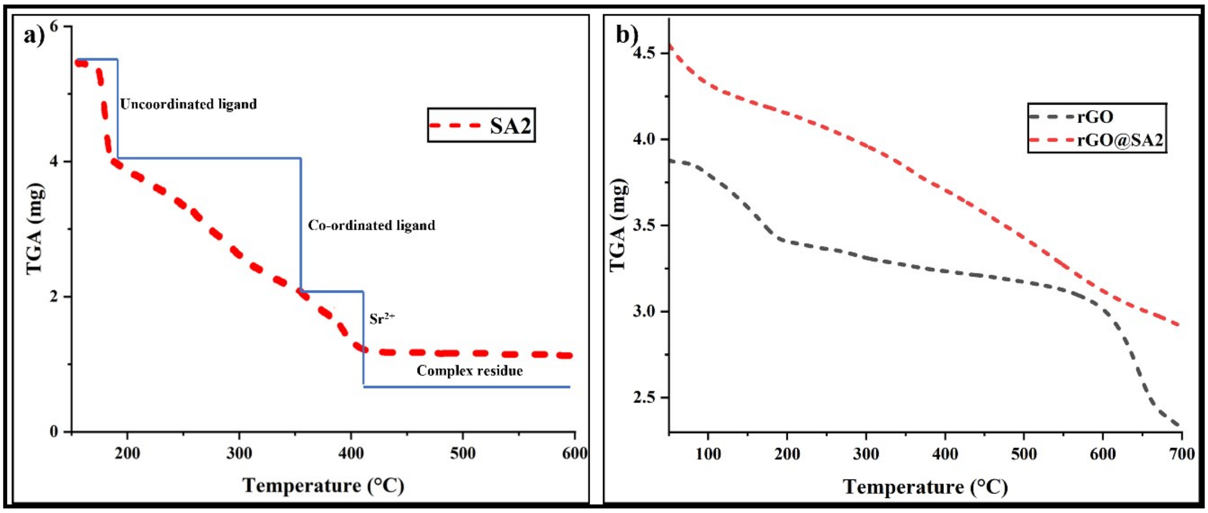

Figure ES3. (a) TGA plot of SA2 and **(b)** TGA plot of rGO and rGO@SA2

8. ^{13}C NMR SPECTRUM

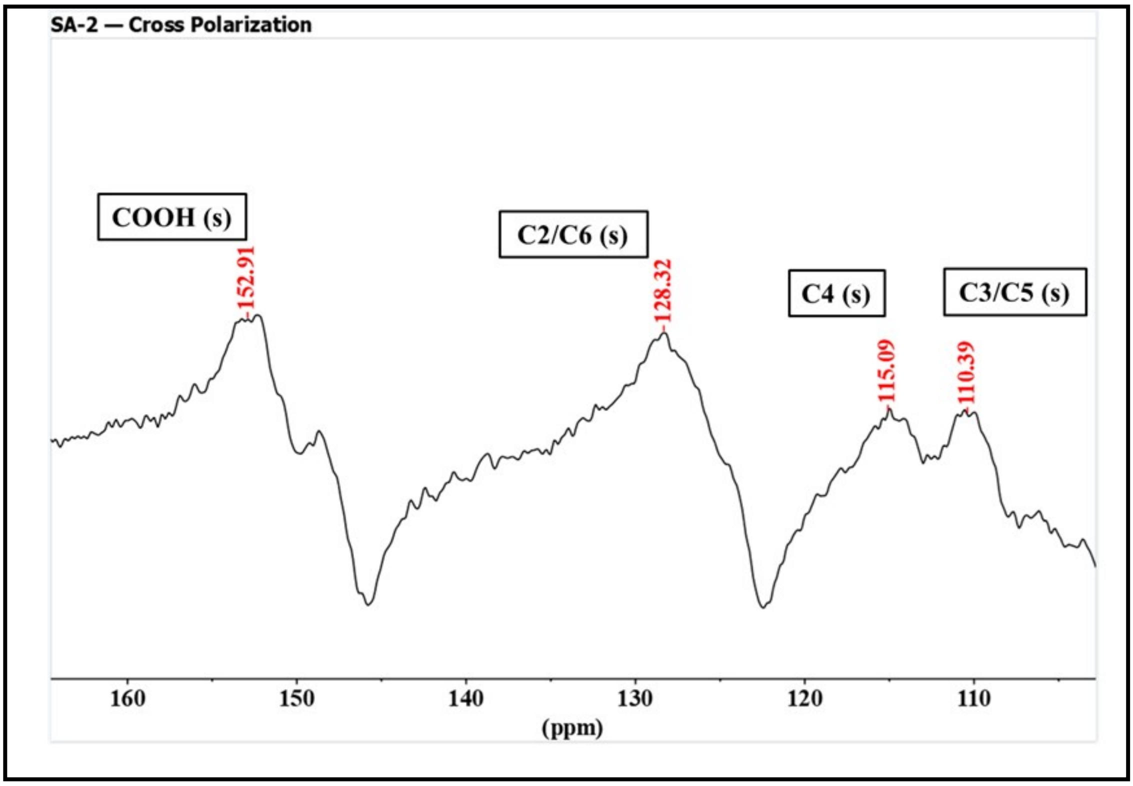

Figure ES4. Solid state ^{13}C NMR spectrum of SA2

9. Table ES2: Bond Lengths for SA2.

Atom	Atom	Length/Å		Atom	Atom	Length/Å
Sr1	O3^1	2.5728(13)		O2	C1	1.259(2)

Sr1	O3^{2}	2.7270(13)		O4	C5	1.255(2)
Sr1	O1^{3}	2.5892(12)		N1	C6	1.339(2)
Sr1	O2	2.5396(13)		N1	C7	1.340(2)
Sr1	O4^{2}	2.6404(13)		C1	C2	1.508(2)
Sr1	O6	2.6115(13)		C5	C4	1.506(2)
Sr1	O5	2.5283(16)		C2	C3	1.390(2)
Sr1	N1^{4}	2.8075(15)		C2	C7	1.390(2)
Sr1	C5^{2}	3.0065(17)		C6	C4	1.386(2)
O3	C5	1.251(2)		C3	C4	1.384(2)
O1	C1	1.254(2)				

10. Table ES3: Bond Angle for SA2

Atom	Atom	Atom	Angle/°		Atom	Atom	Atom	Angle/°
O1^{1}	Sr1	O3^{2}	81.19(4)		C5^{3}	Sr1	O4^{3}	24.61(4)
O1^{1}	Sr1	O3^{3}	147.50(4)		C5^{3}	Sr1	O6	73.09(5)
O2	Sr1	O3^{2}	75.75(4)		C5^{3}	Sr1	O5	97.40(5)
O2	Sr1	O3^{3}	86.92(4)		C5^{3}	Sr1	N1^{4}	98.88(5)
O2	Sr1	O1^{1}	95.51(4)		C5	O3	Sr1^{5}	156.68(11)
O4^{3}	Sr1	O3^{2}	116.27(4)		C5	O3	Sr1^{3}	90.33(10)
O4^{3}	Sr1	O3^{3}	48.40(4)		C1	O1	Sr1^{1}	138.08(11)
O4^{3}	Sr1	O1^{1}	161.30(5)		C1	O2	Sr1	140.87(12)
O4^{3}	Sr1	O2	95.41(4)		C5	O4	Sr1^{3}	94.25(10)
O6	Sr1	O3^{2}	70.66(4)		C6	N1	Sr1^{4}	109.68(11)
O6	Sr1	O3^{3}	68.56(4)		C7	N1	Sr1^{4}	130.37(12)
O6	Sr1	O1^{1}	92.25(4)		C7	N1	C6	117.04(15)
O6	Sr1	O2	143.86(4)		O2	C1	O1	124.49(16)
O6	Sr1	O4^{3}	87.83(4)		C2	C1	O1	118.45(15)
O5	Sr1	O3^{2}	133.68(5)		C2	C1	O2	117.06(15)
O5	Sr1	O3^{3}	115.95(5)		O3	C5	Sr1^{3}	65.09(9)
O5	Sr1	O1^{1}	78.06(5)		O4	C5	Sr1^{3}	61.14(9)
O5	Sr1	O2	146.82(5)		O4	C5	O3	122.91(16)
O5	Sr1	O4^{3}	84.50(5)		C4	C5	Sr1^{3}	159.28(12)

O5	Sr1	O6	69.32(5)		C4	C5	O3	118.63(15)
N1^4	Sr1	O3^2	147.87(4)		C4	C5	O4	118.43(15)
N1^4	Sr1	O3^3	118.07(4)		C3	C2	C1	120.34(15)
N1^4	Sr1	O1^1	93.44(4)		C7	C2	C1	121.34(15)
N1^4	Sr1	O2	73.26(4)		C7	C2	C3	118.13(16)
N1^4	Sr1	O4^3	75.29(4)		C4	C6	N1	123.77(17)
N1^4	Sr1	O6	141.44(4)		C4	C3	C2	119.12(16)
N1^4	Sr1	O5	74.67(5)		C2	C7	N1	123.59(16)
C5^3	Sr1	O3^2	92.41(4)		C6	C4	C5	119.80(15)
C5^3	Sr1	O3^3	24.58(4)		C3	C4	C5	121.85(16)
C5^3	Sr1	O1^1	165.27(4)		C3	C4	C6	118.34(16)
C5^3	Sr1	O2	95.73(4)					

11. Table ES4: Fractional Atomic Coordinates (×10^4) and Equivalent Isotropic Displacement Parameters (Å^2×10^3) for SA2. U$_{eq}$ is defined as 1/3 of of the trace of the orthogonalised U$_{IJ}$ tensor

Atom	*x*	*y*	*z*	U(eq)
Sr1	3143.9(2)	8454.2(2)	1260.7(2)	12.14(8)
O3	5337.3(18)	9017.7(16)	8331.9(16)	20.4(3)
O1	7669.3(19)	3320.9(16)	841.3(17)	19.9(3)
O2	6328.9(18)	6218.1(16)	944.1(16)	19.8(3)
O4	7093(2)	9778.7(17)	5914.0(17)	24.5(3)
O6	1475.1(19)	11456.2(18)	255.2(19)	27.3(3)
O5	-389(2)	9259(2)	2616(2)	29.5(4)
N1	7455(2)	3804(2)	6055(2)	19.3(3)
C1	7064(2)	4846(2)	1586(2)	13.1(3)
C5	6358(2)	8701(2)	6759(2)	14.4(4)
C2	7183(2)	5072(2)	3387(2)	13.9(4)
C6	7096(3)	5428(2)	6752(2)	18.1(4)
C3	6816(2)	6743(2)	4143(2)	14.2(4)
C7	7511(3)	3649(2)	4390(2)	17.1(4)
C4	6776(2)	6927(2)	5853(2)	14.3(4)

12. Table ES5: Anisotropic Displacement Parameters (Å^2×10^3) for SA2. The Anisotropic displacement factor exponent takes the form: $-2\pi^2[h^2a^{*2}U_{11}+2hka^*b^*U_{12}+\ldots]$.

Atom	U$_{11}$	U$_{22}$	U$_{33}$	U$_{12}$	U$_{13}$	U$_{23}$

Sr1	15.42(11)	10.32(10)	10.44(11)	-3.72(7)	-4.25(7)	0.17(6)
O3	26.9(7)	20.4(7)	12.0(6)	-10.7(6)	-0.3(6)	-3.2(5)
O1	24.4(7)	15.8(6)	18.8(7)	-2.7(5)	-9.2(6)	-5.7(5)
O2	24.9(7)	18.1(7)	15.0(6)	-1.9(6)	-9.5(6)	2.3(5)
O4	39.3(9)	18.3(7)	15.6(7)	-16.2(6)	-1.9(6)	-0.9(5)
O6	18.9(7)	22.9(7)	37.8(9)	-6.1(6)	-7.4(6)	9.3(6)
O5	23.3(8)	45.2(10)	17.3(8)	-12.6(7)	-1.3(7)	1.5(7)
N1	28.3(9)	14.6(8)	16.1(8)	-5.9(7)	-10.0(7)	3.9(6)
C1	13.1(8)	15.1(9)	11.2(8)	-5.0(7)	-3.2(7)	-0.9(7)
C5	17.9(9)	14.5(9)	12.2(9)	-5.5(7)	-6.5(7)	0.0(7)
C2	15.5(8)	13.7(8)	12.5(9)	-3.9(7)	-5.1(7)	0.1(7)
C6	24.9(10)	19.4(9)	11.4(9)	-8.4(8)	-6.4(8)	0.8(7)
C3	17.7(9)	11.4(8)	13.5(9)	-5.4(7)	-4.6(7)	2.1(7)
C7	22.1(9)	12.5(9)	15.7(9)	-3.9(7)	-6.4(8)	-0.7(7)
C4	16.6(9)	13.7(9)	11.9(9)	-5.9(7)	-2.6(7)	-1.0(7)

13. Table ES6: Hydrogen Atom Coordinates (Å×10^4) and Isotropic Displacement Parameters (Å^2×10^3) for SA2.

Atom	***x***	***y***	***z***	**U(eq)**
H7	7784(3)	2528(2)	3878(2)	20.5(5)
H6	7058(3)	5557(2)	7904(2)	21.7(5)
H3	6600(2)	7724(2)	3507(2)	17.0(4)
H6a	2115(13)	12151(8)	180(20)	40.9(5)
H6b	434(12)	11959(11)	1051(10)	40.9(5)
H5a	-1010(40)	9260(30)	3590(40)	43(8)
H5b	-870(40)	9150(30)	1990(40)	39(8)

14. Table ES7: The values of K_{SV} and LOD of SA2.

Complex	**K_S (litre/mole)**	**LOD mole/litre, (ppm)**
(a.) SA2 - picric acid	6.8 x10^4	1.8 x 10^{-6}, 0.41

(b.) SA2 – 1,4-nitroaniline	4.3 x 10^4	4.4 x 10^{-6}, 0.61
(c.) SA2 - Benzoic acid	1.5 x 10^4	21 x10^{-6}, 2.6
(d.) SA2- Barium salt	4.7 x 10^4	2.2 x 10^{-6}, 0.57

15. Table ES8: Summary of Sr-based CPs used for supercapacitor applications

S. No.	Electrode Materials	Electrolyte	Current Density (Ag^{-1})	Capacitance (Fg^{-1})	Ref.
01.	**Sr MOF** **Cu-doped Sr MOF**	3 M KOH 3 M KOH	1.0 1.0	147.8 443	[51]
02.	**SA2** **rGO** **rGO@SA2**	**1 M H_2SO_4** **1 M H_2SO_4** **1 M H_2SO_4**	**0.5** **0.5** **0.5**	**153.57** **349.38** **383.38**	**This work**

16. rGO CV and GCD graph

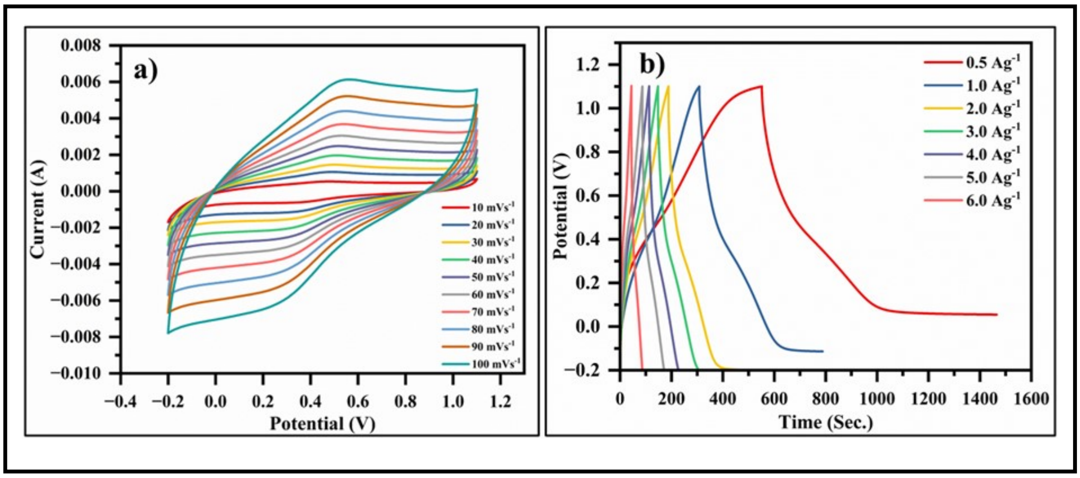

Figure ES5. CV and GCD curve of rGO

References:

1 O. V. Dolomanov, L. J. Bourhis, R. J. Gildea, J. A. K. Howard and H. Puschmann, *J. Appl. Crystallogr.*, 2009, **42**, 339–341.

2 L. J. Bourhis, O. V. Dolomanov, R. J. Gildea, J. A. K. Howard and H. Puschmann, *Acta Crystallogr. Sect. A Found. Adv.*, 2015, **71**, 59–75.

3 V. A. Blatov, A. P. Shevchenko and D. M. Proserpio, *Cryst. Growth Des.*, 2014, **14**, 3576–3586.

4 M. O’Keeffe, M. A. Peskov, S. J. Ramsden and O. M. Yaghi, *Acc. Chem. Res.*, 2008, **41**, 1782–1789.

5 E. V. Alexandrov, A. P. Shevchenko and V. A. Blatov, *Cryst. Growth Des.*, 2019, **19**, 2604–2614.

6 K. Lyu, Y.-L. Wei, Y.-H. Li and G.-H. Cui, *J. Mol. Struct.*, 2021, **1225**, 129128.

7 K. Bauri, B. Saha, J. Mahanti and P. De, *Polym. Chem.*, 2017, **8**, 7180–7187.

8 R. Ahmed, A. Ali, M. Ahmad, A. Alsalme, R. A. Khan and F. Ali, *New J. Chem.*, 2020, **44**, 20092–20100.

9 Q. Ma, F. Cui, M. Liu, J. Zhang and T. Cui, *Nanoscale*, 2021, **13**, 11112–11119.